1986

# Performance Predictions and Test Results of a Free Piston Stirling Engine Driven Heat Pump

D. O. Jones

R. J. Vincent

G. Pfleiderer

# PERFORMANCE PREDICTIONS AND TEST RESULTS OF A FREE-PISTON STIRLING ENGINE DRIVEN HEAT PUMP

D. Jones, R. Vincent, G. Pfleiderer

MECHANICAL TECHNOLOGY INCORPORATED
968 Albany-Shaker Road, Latham, NY 12110

## ABSTRACT

Recent progress on a Stirling engine driven heat pump is described and a modeling technique for predicting engine dynamics is developed. The system described represents a very promising configuration of engine driven heat pump, because of the long life characteristics of the free-piston Stirling engine and the hermetic nature of both the engine and refrigerant working fluids. Recent changes in the transmission of this system and the design of a new engine section have allowed performance to become very attractive. With planned development of the Mark I, demonstration of the system's commercial potential and eventual field testing of prototype units will be forthcoming.

## INTRODUCTION

The area of engine driven heat pumps for residential use has been receiving increased attention, with several organizations in the US and Japan attempting to develop marketable systems. Mechanical Technology Incorporated (MTI), with the joint sponsorship of Gas Research Institute and the Department of Energy through a subcontract to Oak Ridge National Laboratory,* is developing a heat activated heat pump (HAHP) of 3 Refrigeration-Ton (RT) cooling capacity, based on the free-piston Stirling engine (FPSE). The Stirling engine, either free-piston or kinematic, is an excellent choice as prime mover because of its quiet operation, long life potential, and ability to burn many fuels cleanly in an external combustion system.

* The ongoing guidance, review, and support of George T. Privon and Dr. J. Michael Clinch of Oak Ridge National Laboratory and Gas Research Institute, respectively, is gratefully acknowledged.

The free-piston Stirling engine has the further advantage of being hermetically-sealed. It is also easily modulated and readily coupled to a reciprocating compressor by means of a flexible diaphragm barrier and oil-filled transmission. The refrigerant system is then also hermetic, with the exception of small quantities of oil which can leak past shaft seals and into the refrigerant. This oil is easily separated, collected, and pumped back into the transmission. The current configuration of the HAHP, termed the Mark I, is shown in Figure 1. A photograph of the HAHP without external piping or instrumentation leads is shown in Figure 2. It will be described in more detail following a description of the basic operation of a free-piston Stirling engine.

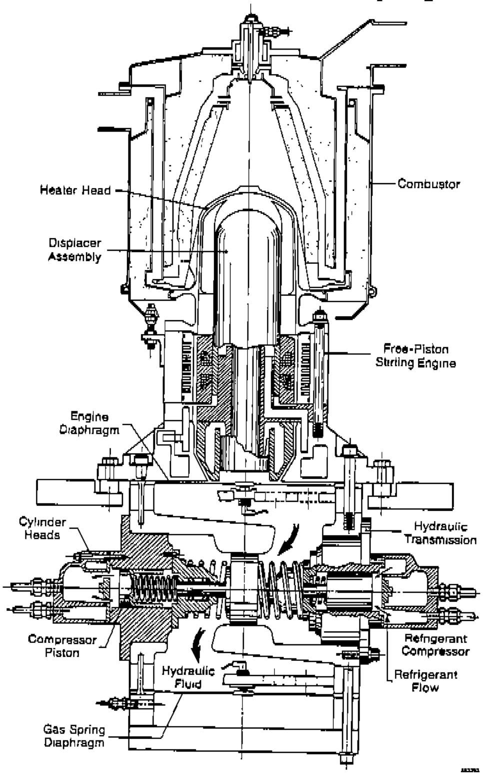


Fig. 1 Mark I Heat Pump

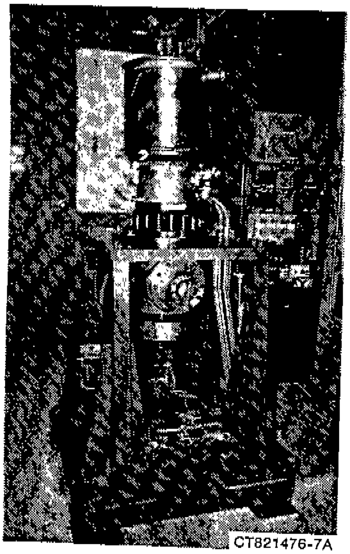


Fig. 2 Heat Pump Installed in Test Cell

The FPSE normally uses two moving pistons that cyclically compress, heat, expand, and cool a working fluid which, in this case, is high pressure helium. A nearly sinusoidal pressure wave is generated in the engine that lags the motion of the power piston and transfers PV power to it. This power is typically extracted by a linear electric alternator using magnets on the piston or a piston-driven compressor that is contained within the pressure boundaries of the engine.

When the working gas is displaced by motion of the displacer piston, it passes through three heat exchangers in series - the heater, regenerator, and cooler. The heater region is usually kept at 720-800°C and the cooler at 10-50°C. The regenerator, a critical component made of a porous metallic medium such as fine wire stacked screen, prevents the inefficient transfer of heat from the heater to the cooler by extracting heat from the gas during one part of each cycle, storing it, and returning that heat to the gas during the second part of each cycle. In the design of regenerators, the desired high heat transfer properties of a matrix are countered by excessive pressure drop loss if, for example, the regenerator is too long or too densely packed.

All Stirling engines operate on the principles described above. The FPSE is a resonantly-oscillating machine in which the two moving parts, the piston and the displacer, are not connected to any linkage arrangement. The phasing and strokes of these members are determined by the interaction of gas spring forces, thermodynamic power transfer, load applied to the piston, and electric control power that aids in driving the displacer. Mechanical friction is eliminated by the use of clearance seals and hydrostatic gas bearings, supplied internally by tapping small quantities of gas from one of the gas springs. Figure 3 is a photograph of the Engineering Model (EM) FPSE, 3-kW electric, which was designed and built in 1982 (Ref. 1). The engine has a mean internal pressure equal to 60 Bar and operates at 60 cps, parameters which are approximately the same in the HAHP.

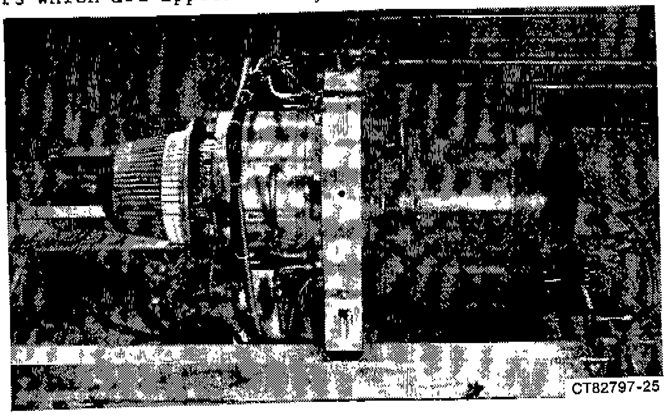


Fig. 3 EM Engine Installed for Endurance Test

The kinematic Stirling engine (KSE) is used when shaft power is desired. One configuration that displays high power density is a four cylinder, double-acting engine called the Rinia arrangement. MTI, in cooperation with United Stirling of Sweden, has developed two models of a high performance KSE that are suitable for automotive use. The latest configuration (Ref. 2) is a V-4 with single crankshaft and simplified heat exchangers. Design emphasis was placed on reduced size, weight, and manufacturing cost. Several other applications for these engines are also under investigation.

This paper will describe the critical components of the free-piston HAHP and discuss the measured performance obtained to date as well as the performance improvements expected for the Mark I. The paper will also describe the analytical technique developed for predicting steady-state operating dynamics of the engine, given a known piston stroke and load. The computer code which performs this analysis is outlined, along with the MTI thermodynamic code used in conjunction with the dynamic analysis. Several examples of the use of the code are given and results are compared to test data.

## HEAT PUMP CRITICAL COMPONENTS

### 1. Direct-Acting Transmission

The HAHP transmission is oil-filled and relies on the motion of the oil to couple diaphragm deflection to piston motion. Diaphragm center deflection somewhat greater than .2-inch is used to obtain a much longer maximum compressor stroke.

The mass of the reciprocating piston assembly is 16.5 lbm, and at maximum stroke, the resulting shaking force is more than 2000 lbf. Unless the compressor case is very heavy, case vibration will be excessive. Experience has shown that vibrations at the combustor must be less than 1 g to allow long life. As initially designed and tested (Ref. 3 and 4), the HAHP transmission included an oil-driven counterweight, also weighing 16.5 lbm, that moved in opposition to the piston and thereby eliminated compressor shaking forces at all strokes and frequencies. Final performance testing of this configuration, completed in early 1985, showed that unavoidable oil viscous losses associated with the counterweight could exceed 1000 watts at high strokes, and overall transmission loss could approach 1500 watts. With the counterweight removed and minor changes made to streamline the oil flow, transmission loss fell to approximately 400 watts at high stroke. Figure 4 gives some of the data on transmission power loss with and without the counterweight. Currently, measured transmission efficiencies are greater than 85% at medium to high power levels. Further improvement in transmission efficiency is expected when planned design changes are incorporated.

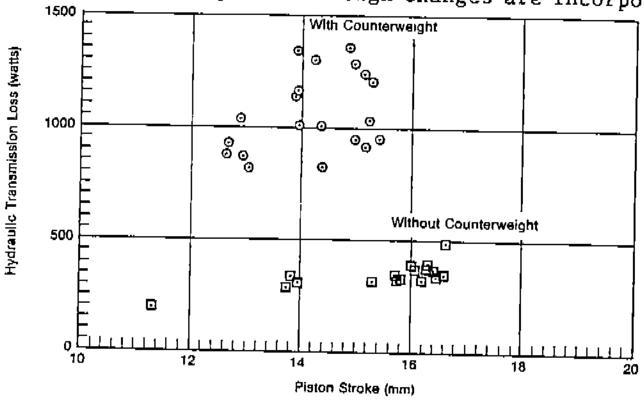


Figure 4

Breadboard Transmission Power Loss

The problem of high shaking force in the direct-acting transmission was solved by designing an external, tuned vibration absorber system for attachment to the transmission case. This approach was taken because, ideally, the HAHP is a constant frequency machine. Tuned vibration absorbers are known to be particularly useful in fixed frequency applications. In practice, small variations in frequency are needed to obtain optimum tuning at all refrigerant conditions, but the system has been shown to tolerate up to 4 Hz of variation without excessive vibration. The vibration absorbers currently in use are described below.

## 2. External Vibration Absorbers

The vibration absorber system consists of two 35 lbm assemblies attached by means of leaf spring packs to the right and left sides of the compressor housing. The absorbers oscillate with maximum stroke equal to .2-inch and generate forces at their attachment points to the case that are equal and opposite to the inertia force produced by the internal piston assembly. With the absorbers tuned to match the system's operating frequency, case acceleration becomes zero for any value of piston stroke (Ref. 5). Figure 5 presents a summary of the system design features and a schematic drawing of the absorbers as mounted to the sides of the case. Figure 6 is a detail of the right side absorber showing the two leaf spring packs, with spacers, and the support brackets used to distribute loads to the transmission case.

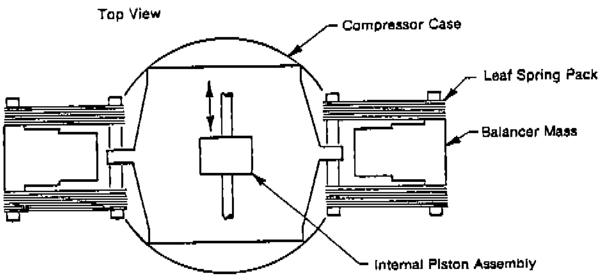


**Balancer Specifications**

| | |
|---|---|
| Balancer Dynamic Mass | 38 $lb_m$ (each side) |
| Case Effective Mass | 285 $lb_m$ |
| Unbalance Force, F | 2442 $lb_f$ – 57.8 Hz,<br>Due to 16.5 $lb_m$ Piston at 22-mm Stroke |
| Leaf Springs | 13 Springs Per Pack; 17-7 PH 0.071-in Sheet |
| Maximum Bending Stress | 35 ksi at Stroke = 0.204 in. |

**Performance on GRI/DOE Heat Pump**

| | |
|---|---|
| Tuned Operating Point | 57.8 Hz |
| Operating Frequency Range | 54 to 60 Hz |
| Case Lateral Acceleration | < 1.5 g at 56 Hz |
| Combustor Lateral Acceleration | < 0.3 g at 56 Hz |

Fig. 5 Schematic of Vibration Absorbers

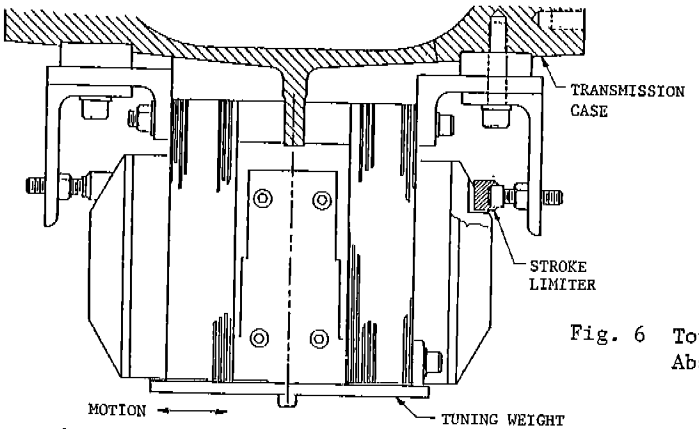


Fig. 6 Top View of Absorber

Extensive structural analysis of the attachment scheme and leaf spring design was performed prior to establishing a final design, but this will not be covered here. In addition, a six degree-of-freedom dynamic model was prepared which modeled independent motion of the two absorbers, and lateral and rotational motion of the case and test stand. Even when tuning is not the same for both absorbers, no difficulties were seen with unequal strokes, out-of-phase operation, or beating between modes. In practice, operation of the absorbers has been trouble free over an accumulated operating time exceeding 300 hours. Tear-down and inspection of the leaf springs and spacers will reveal if development efforts are needed to reach the design life of 50,000 hours.

3. Diaphragms

Two high-strength steel diaphragms having contoured cross-section are currently used in the HAHP. This diaphragm configuration, pictured in Figure 7a, allows much larger volume deflections than does a flat plate diaphragm before metal stresses exceed fatigue endurance limits. The contoured design has proved quite successful over two years of testing, but at least 20% greater volume capability is desired for increased engine power. Alternatives are being considered.

Two performance criteria are applicable to the diaphragm selection - 1) high volume deflection at relatively low stress, preferably with reduced working diameter; and 2) high centering stiffness so that substantial mean pressure differences across the diaphragm (1 to 2 psig) will not cause excessive offset or bias. Two alternatives which show promise for replacing the contoured diaphragm are shown in Figures 7b and 7c. These are the convoluted diaphragm often used where highly linear deflection behavior is required and the articulated diaphragm developed in England (Ref. 6). A fourth candidate, especially useful when small diameter is needed, is the welded metal bellows with auxiliary centering spring. However, the cost of such a system may be relatively high for any production model of residential heat pump. Analysis of several diaphragm designs in each style is currently in progress.

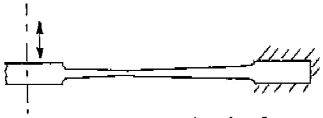

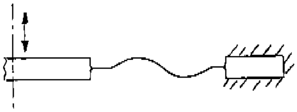

Fig. 7a Contoured Diaphragm Fig. 7b Convoluted Diaphragm

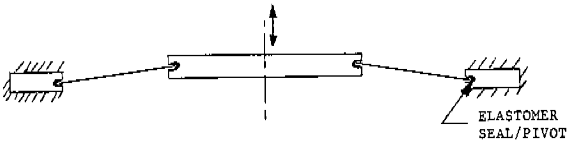


Fig. 7c Articulated Diaphragm

## 4. Oil Management System

The oil management system can be thought of as performing two functions: 1) maintain both the engine and gas spring diaphragms on center; and 2) collecting, separating, and reinjecting any transmission oil which leaks past the high pressure chevron seals. In the case of diaphragm centering, the oil management system must also balance the mean gas pressures in the engine working space and the lower gas spring. Currently, sensors are employed to measure the deflection of both diaphragms, and an electronic logic system compares diaphragm mean position to pre-determined midstroke values. If correction is needed, the oil management system causes four solenoid valves to operate as required. These valves either 1) charge or discharge high pressure oil into the transmission cavity, controlling the 'bulge' of the diaphragms; or 2) charge or discharge high pressure gas into the lower gas spring, controlling the coupled downward or upward deflection of the diaphragms. Reliable, automatic operation of this system has been seen over nearly two years of testing, but the cost of sensors and solenoid valves may be prohibitive in a production HAHP. Passive systems with inherently low cost are being evaluated as eventual replacements for the existing electronic system. The development of an inexpensive oil management system will be eased if diaphragm centering stiffness is relatively high. For this reason, extremely flexible diaphragms, which may allow large volume deflections, are not considered useful in this application.

The function of oil separation and reinjection is accomplished by using an oil separator bottle and an inexpensive, high-pressure gear pump driven by a fractional horsepower motor. As accumulated oil leakage is sensed, the pump is periodically activated for 10 to 20 seconds. This maintains sufficient oil in a high pressure accumulator for charging the transmission cavity when required. Oil compatibility with refrigerants was checked before beginning a series of tests with various transmission oils. Selection of an acceptable, low viscosity transmission oil has been narrowed to either a 10 cS silicone oil or a less expensive 10 cS mineral oil. A 2 cS silicone oil was also tested, but its high cost does not appear justified by the small measured improvement in efficiency.

## HEAT PUMP PERFORMANCE RESULTS

Following initial check out tests of the direct-acting compressor with vibration absorbers, an extensive test series was accomplished to fully characterize the behavior of the Breadboard system. This system included an engine based on EM hardware, redesigned to fit the HAHP lower end. Table I gives the refrigerant suction and discharge test conditions, and Figure 8 shows some of the flow rates measured during the various tests. Heat pump capacity was modulated by controlling the displacer stroke. Maximum capacity reached at 95°F conditions was 2.5 RT, but this is expected to increase during early development of the Mark I. For the three low temperature conditions shown in Figure 8, compressor load was quite small because of the low suction gas density, and the machine was not power limited. High piston strokes were not run at these points because of deflection limitations imposed by the diaphragms.

| | COOLING | | | | HEATING | | | | |
|---|---|---|---|---|---|---|---|---|---|
| | 95°F | 87°F | 80°F | Test Pt2 | 47°F | 32°F | 17°F | 0°F | Test Pt1 |
| DISCHARGE PRESSURE (psia) | 277.4 | 225.5 | 196.5 | 311.5 | 210.6 | 202.1 | 196.5 | 183.1 | 241.0 |
| SATURATION TEMPERATURE (°F) | 121 | 105 | 95 | 130 | 100 | 97 | 95 | 90 | 110 |
| SUCTION PRESSURE (psia) | 90.7 | 94.7 | 98.7 | 90.7 | 76.2 | 57.7 | 42.9 | 29.8 | 69.6 |
| SATURATION TEMPERATURE (°F) | 45 | 47.5 | 50 | 45 | 35 | 20 | 5 | -12 | 30 |
| SUCTION TEMPERATURE (°F)* | 55 | 57.5 | 60 | 55 | 45 | 30 | 15 | -2 | 40 |
| PRESSURE RATIO | 3.06 | 2.38 | 1.99 | 3.43 | 2.76 | 3.50 | 4.58 | 6.14 | 3.46 |

*Includes at least 10°F Superheat

Table I Refrigerant Test Conditions

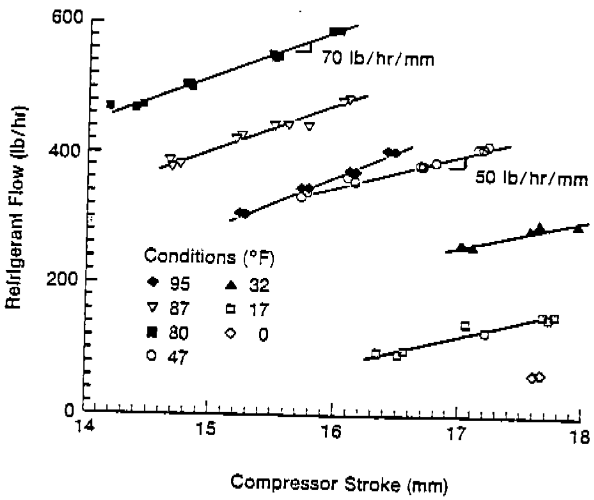


Fig. 8 Refrigerant Flow Rates vs. Stroke

Figure 9 shows the capacities plotted versus the various ambient temperatures and also gives the load line (heating and cooling) for a typical four bedroom home in the mid-Atlantic region. Ideally, the heat pump will be fully modulating and follow the load line without on/off control. Development efforts direct toward achieving improved modulation will involve testing at lower than three-quarter displacer stroke and possible reduction of heater head temperature for some operating points.

Figure 10 compares the heat pump's compressor COP at various ambient temperatures to the equivalent quantity for advanced electric heat pumps. In the figure, engine or motor efficiency is not included, and no credit is taken for engine rejected heat in the heating mode. The figure shows that the lower end performance is very good. Figure 11 shows the predicted COP for the Mark I system, assuming 25% engine efficiency based on fuel higher heating value and crediting the system with 85% of engine heat rejected at the cooler. The Bread-board engine displayed efficiencies considerably lower than 25%, but the causes have been identified and are being addressed in the Mark I. Engine efficiencies of at least 30% are projected for future, optimized designs. Achieving the high COP's shown with the Mark I heat pump and obtaining 3.0 RT capacity will clearly aid in demon-strating the potential of this approach for commercial applications.

## SYSTEM DYNAMIC ANALYSIS

Dynamic analysis of the engine/compressor system was required from the beginning of the concept design through the development of the Mark I. The HAHP represented the first successful coupling of an

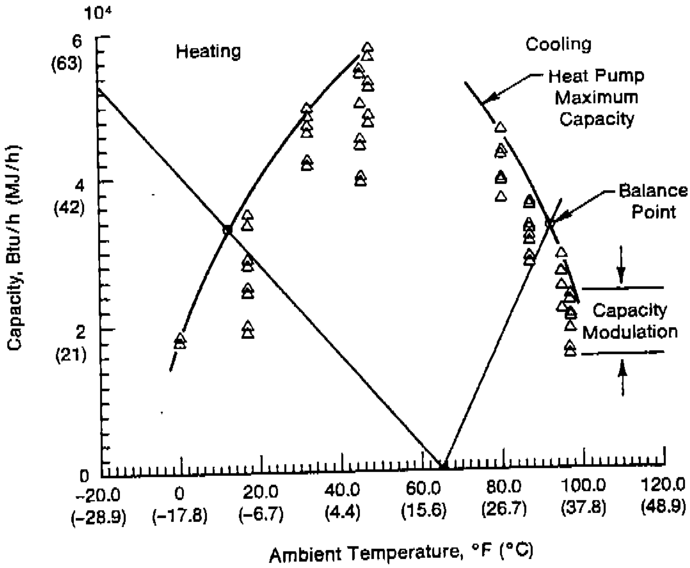


Fig. 9 Heat Pump Capacity vs. Ambient Temperature

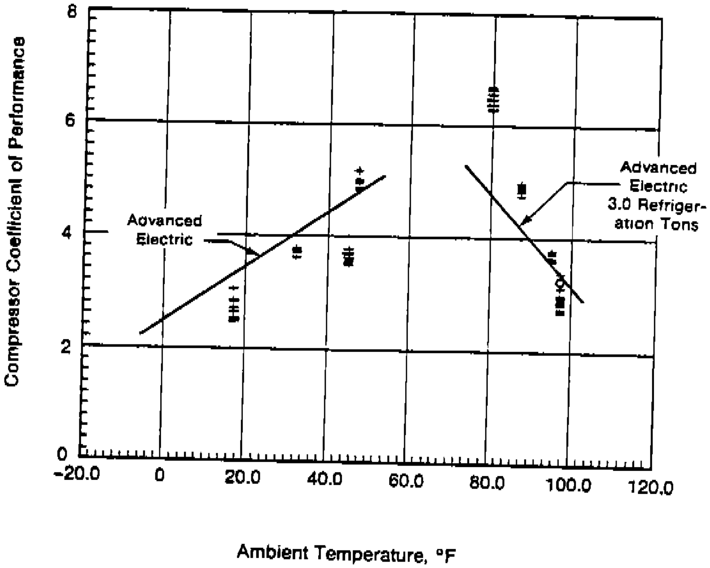


Fig. 10 Compressor Coefficient of Performance

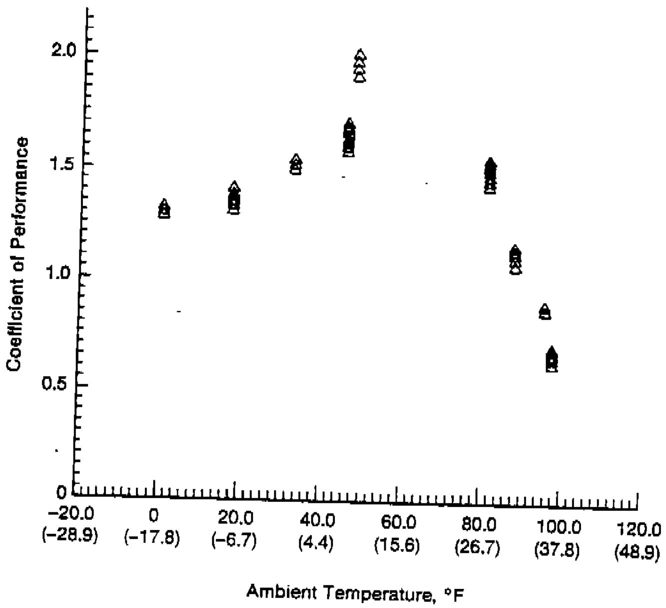


Fig. 11 Heat Pump COP's for 25% Engine Efficiency

FPSE to a refrigerant compressor. The initial decision to build the Breadboard system for concept evaluation and developmental testing required analytical predictions that such a system could operate stably and achieve performance goals over a wide range of ambient load conditions. To understand and evaluate the dynamic characteristics of an engine/compressor system, a coupled dynamic/thermodynamic model of the system was developed. A brief description of the dynamic model and its interaction with the thermodynamic model is presented below.

## Development of the Dynamic Model

The MTI Stirling engine thermodynamic code (Ref. 7) is a rigorous, fast running, harmonic code with up to 20 control volumes. The code calculates engine pressures, heat flows, losses, power, and efficiency as a function of engine geometry, gas properties, temperature, and four specified quantities that are actually determined by dynamics or engine-to-load coupling characteristics. These quantities are: 1) frequency, 2) displacer stroke, 3) displacer phase angle relative to piston, and 4) piston stroke. The dynamic model developed here is a technique for combining the thermodynamics with dynamics to predict the operating point of a free-piston Stirling engine. Other more involved dynamic/thermodynamic models, not covered in this discussion, have been used at MTI for stability and transient analysis.

Engine power is given by:

$$\mathbb{P} = \pi f \; P_c \; A_p \; X_p \; \sin \Theta \tag{1}$$

Where:
- $\mathbb{P}$ = indicated power (watts)
- $f$ = operating frequency (Hz)
- $P_c$ = compression space pressure amplitude (N/m)
- $X_p$ = power piston amplitude (m)
- $A_p$ = power piston area ($m^2$)
- $\Theta$ = phase lag between pressure amplitude and piston motion (degrees)

In phasor diagram form, the compression space pressure relative to piston and displacer motion is represented by:

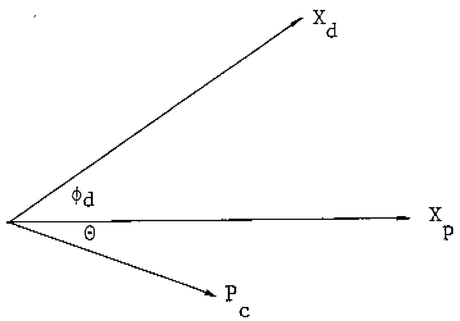

Note that the quantitiy $P_c A_p \sin \Theta$ represents the component of the pressure force that acts in phase with the piston velocity, transferring power to the load.

Representing $P_c$ as a vector made up of two components, one in phase with piston motion and one out of phase with displacer motion yields:

$$P_c = P_{fp} X_p + P_{fd} X_d$$

In phasor diagram form, the $P_c$ representation is as follows:

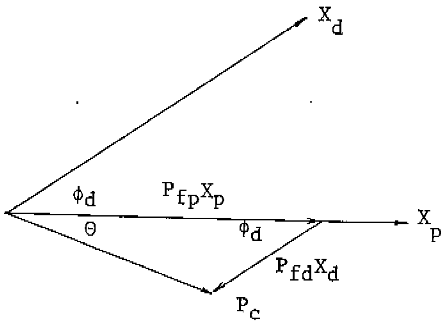


Note that:

$$P_c A_p \sin \Theta = P_{fd} X_d A_p \sin \phi_d \qquad (2)$$

Substituting into equation (1) yields:

$$\mathbb{P} = \pi f \, P_{fd} X_p X_d A_p \sin \phi_d \qquad (3)$$

which correctly correlates the engine 'dynamic quantities' $X_d$, $X_p$, $f$, and $\phi_d$ with the thermodynamic quantity $P_{fd}$, yielding engine power.

Engine dynamic quantities $X_d$, $X_p$, $f$, and $\phi_d$ can be computed from force balances on both the power piston and the displacer.

Power Piston Force Balance

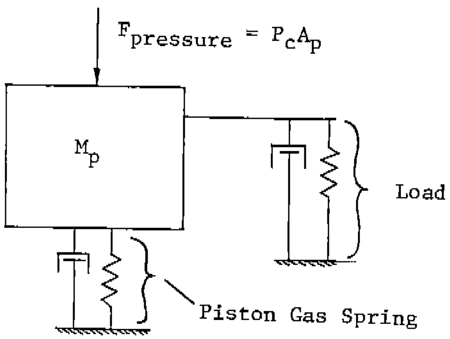

$$F_{pressure} + F_{spring} + F_{load} = F_{inertia}$$

$$M_p\omega^2 X_p + C_{total}\omega X_p + k_{total}X_p = F_{pressure}$$

Representing these forces in phasor diagram form yields:

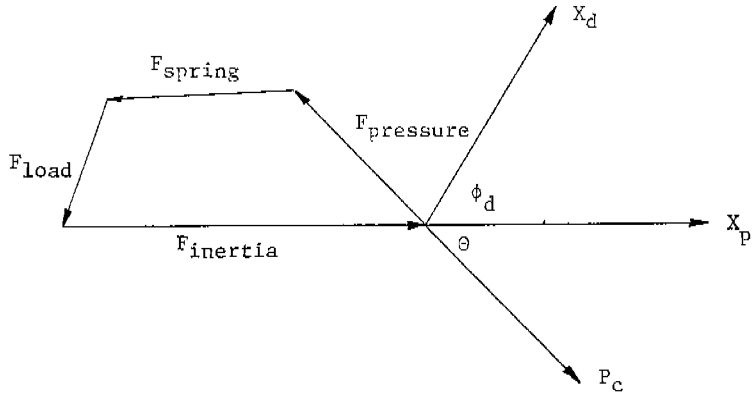


Equating vertical and horizontal components yields:

$$C_{total}\omega X_p = F_{pressure} \operatorname{Sin} \Theta \tag{4}$$

$$M_p\omega^2 X_p = k_{total}X_p + F_{pressure} \operatorname{Cos} \Theta \tag{5}$$

By rearranging and dividing these equations, we obtain:

$$\phi_d = \tan^{-1}\left[\frac{\omega \quad C_{total}}{P_{fp} \; A_p + k_{total} - M_p \; \omega^2}\right] \tag{6}$$

and

$$X_d/X_p = \omega \; C_{total} \; / \; P_{fd} \; A_p \operatorname{Sin} \phi_d \tag{7}$$

In practice, both $X_p$ and frequency are fixed, and equations (6) and (7) are applied to find values of $X_d$ and $\phi_d$ which are consistent with the defined load ($C_{total}$). The thermodynamic model of the engine automatically iterates with the dynamic model to produce thermodynamic quantities $P_{fp}$ and $P_{fd}$ which are consistent with the dynamic quantities $X_d$ and $\phi_d$. Convergence is determined by comparing values of $X_d$ and $\phi_d$ employed in the thermodynamic analysis with values calculated in the dynamics.

## Application

The code results have been compared to laboratory test data for the cases of 1) fixed ambient temperature condition (i.e., refrigerant suction and discharge pressure) at various piston strokes, and 2) fixed piston stroke at various ambient temperature conditions. For each of the cases considered, engine measurements for displacer stroke and displacer phase angle are correlated with code prediction.

Figures 12 and 13 present the measured data and code predictions for 95°F ambient load conditions at various piston stroke levels. Since the compressor load conditions are set and controlled by the refrigerant flow loop, compressor flow rate becomes a function of compressor stroke only. Compressor stroke is controlled by the amount of engine power which is delivered, and this can be modulated via the displacer stroke. Thus, by controlling displacer stroke, refrigerant flow rate and heat pump capacity are modulated. The figures present data for normalized displacer stroke modulation between three-quarter and full stroke, resulting in piston stroke variation from 15 to 16.5 mm and capacity modulation from 22,000 to 29,000 BTU/hr. Code correlation was first performed by developing a match point about the .81 displacer stroke point. Engine volume was adjusted slightly and effective oil mass was adjusted to force the match indicated. Once the match point was established, the code was applied to predict displacer stroke and phase angle for the two other compressor piston stroke levels. The code is shown to closely follow the displacer strokes and phase angles of the data. If the match point correlation for phase angle had been forced closer than the 2% type agreement shown, better correlation at the higher and lower stroke levels would have resulted.

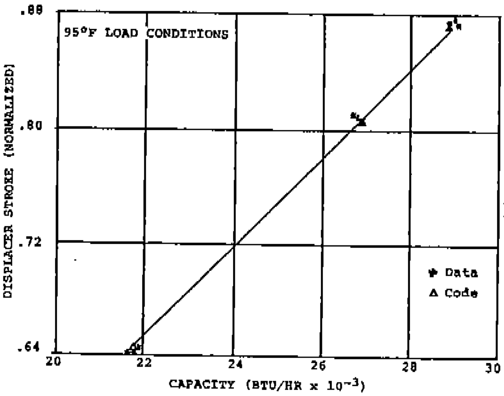


Figure 12

Displacer Stroke vs Capacity (Data and Code at 95°F)

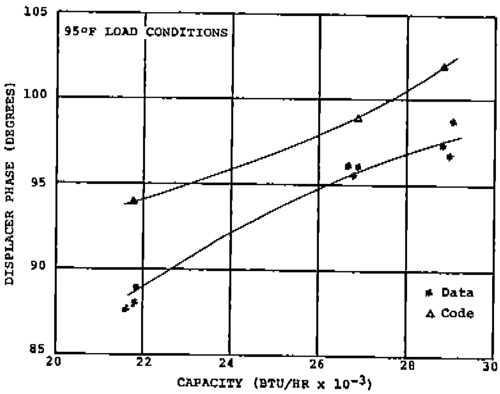


Figure 13

Displacer Phase vs Capacity (Data and Code at 95°F)

Figures 14 and 15 represent 17, 47, 80, and 95°F compressor load conditions for fixed piston strokes of 16 mm. Again, refrigerant capacity is plotted versus displacer stroke and displacer phase angle. The code results show a close match with measured displacer stroke but correlates more poorly with displacer phase angle. As engine power is a function of the sine of the phase angle, this mismatch is not considered critically significant. However, closer agreement should have been expected. Slight changes in engine mean pressure and temperature ratio are probable causes which may explain the discrepancies.

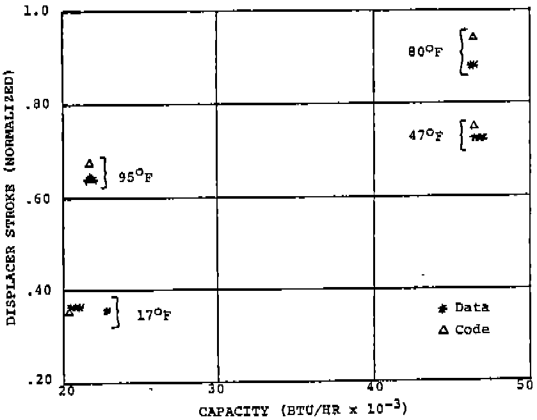


Figure 14

Displacer Stroke vs. Capacity (Various Ambients)

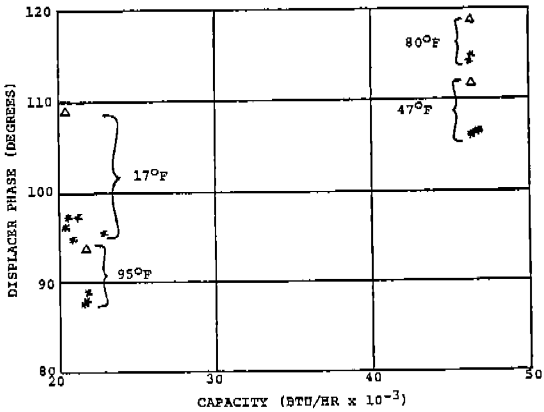


Figure 15

Displacer Phase vs. Capacity (Various Ambients)

The coupled dynamic/thermodynamic model is used for predicting the effect of various tuning changes on the system. Several techniques have been proposed for obtaining increased power from the FPSE, and these are currently being analyzed. The objective is to develop a heat pump of 3 RT capacity (95°F conditions) which has high COP, can achieve high refrigerant flow at 17°F conditions, and is highly modulating. The Mark I heat pump, with careful analysis and testing of the components affecting dynamics and efficiency, will represent a major step toward a production prototype model to determine marketability.